Isomorphic transformation of the Lorenz equations into a *single*-control-parameter structure

Belkacem Meziane

Université d'Artois, UCCS Artois, UMR CNRS 8181, Rue Jean Souvraz, SP18, 62307 Lens Cedex, France

Abstract— *An isomorphic structure that converts the Lorenz equations, whose dynamic properties are usually described in terms of three independent factors, into a single control-parameter system, is put forward and analyzed. Such an isomorphism is shown to bring an intrinsic simplification that offers much better depictions of the Lorenz non-linear dynamics, while it allows for quicker and forthright inspection of the control-parameter domains, inside which well-defined periodic, both symmetric and asymmetric, as well as chaotic solutions occur.*

Keywords— Lorenz equations, Fluid turbulence, Laser theory, Instabilities and chaos, Nonlinear dynamics

I. INTRODUCTION

After decades of intensive attention since their initial derivation in fluid turbulence [1], and their analogy with Laser Physics [2], which resulted in hundreds, most likely thousands of contributions, including entire books and book chapters [3, 4], the Lorenz equations still remain one of the challenging problems, from both the mathematical and the physical points of view. On the one hand, physicists have been mainly concerned with experimental demonstrations that would eventually display deterministic low-dimensional chaotic behavior, in fluid turbulence [5] as well as in coherent-light-matter interactions [6]. On the other hand, mathematicians have dedicated extensive efforts towards computer assisted proofs pertaining to the existence of the so called Lorenz attractor [7-10]. These equations, whose unstable dynamics is governed by three control parameters, exhibit a rich variety of solutions. Yet, it appears that, for historical reasons, the barycenter of attraction spins around narrow zones of the large control-parameter domains, be it in fluid turbulence or in the nonlinear laser-matter-interaction issue. For instance, numerous investigations devoted to fluid dynamics mostly paid attention to the initial set of parameters that was put forward by Lorenz in his primary work, while laser physicists concentrated their efforts on effective constraints that typically yield periodic solutions.

It is also worth recalling that despite the huge amount of published reports that dealt, and continue to deal with Lorenz dynamics [11-16]; in terms of their mathematical properties, no particular connection between the innumerable results has ever been put forward, leaving one lone justification to each exotic report, which always associates to the unpredictable nonlinear nature that connects the three interacting variables. As a consequence, the reported data seems to go along some quite irregular sequences similar to the chaotic nature of these nonlinear equations. The lone and overall evidence that could somehow be extracted when digging into the countless publications is the fact that, for some control parameters, the solutions exhibit periodic time traces, that deviate into some hierarchical cascading with the increase or decrease of some external excitation level, while for others, the solutions become chaotic, with erratic trajectories, that depict some sort of "strange attractors" when represented in the associated phase space. Probably, the search for any generic law in the solution-structures has been left aside because of the fact that the primary concern has, in most cases, been devoted to the demonstration of deterministic chaos in experimental systems, and the proof of existence of the Lorenz attractor, from a mathematical point of view [7-10]. To the best of our knowledge, no generic study has ever been undertaken to give a complete synopsis of the Lorenz equations, out of which one might precisely forecast its unstable solutions, given the values of its control parameters.

The purpose of the present paper is threefold. Its primary objective is to demonstrate, for the first time, that the solutions of the Lorenz equations possess some repeatedly organized and systematic properties that allow for straightforward identification of its periodic windows, asymmetric and chaotic solutions, following some functional arrangements of its control-parameter values. Based on such endorsement, a second step will naturally end-result to transforming the Lorenz equations into a single control-parameter set that encloses the same abundant dynamical solutions, while preserving the full hierarchies and features of the three-control-parameter system. As a final outcome, a summarizing generic map is given to sum up the predicted solution-windows associated with the single control-parameter range values, with the expectation that such a noteworthy simplification will render its hidden properties much easier to apprehend. First, let us give a quick reminder of the Lorenz equations, along with the main features of their solutions.

II. OUTLINE OF THE LORENZ-EQUATIONS MAIN-CHARACTERISTICS

It took twelve years before the original Lorenz equations were accredited a one to one correspondence with the semi-classical theory that describes the nonlinear light-matter interactions that take place inside a unidirectional ring laser cavity operating in single mode and homogenously broadened amplifying medium. When the three interacting variables are normalised to their steady-state values, a set of three non-linearly coupled differential equations is derived to take the following basic structure [2, 4, 6, 15, 16]

$$\partial_t X = -\kappa\{X + \rho Y\} \tag{1a}$$

$$\partial_t Y = -Y + XZ \tag{1b}$$

$$\partial_t Z = -\wp\{Z + 1 + XY\} \tag{1c}$$

Where *X(t)* is the electric field, *Y(t)* the polarization and *Z(t)* the population inversion of the amplifying medium.

Three control parameters appear in the above system: The excitation parameter ρ, which quantifies the level of some external pumping mechanism that transforms an initially absorbing material into an amplifying medium, the electric field decay rate κ, and the population inversion relaxation rate $\wp$. For simplifying purposes, both decay rates are scaled to a polarisation relaxation rate, which naturally disappears from the initial equations [For details, see Ref. 4].

In the bad cavity configuration (for which the cavity decay rate exceeds the sum of the population inversion and polarisation decay rates), and beyond some critical pumping level ρ_{2th} (so-called second laser-threshold, or instability threshold), the above equations become unstable, revealing a rich variety of more or less complex solutions, in the form of regular and irregular, quite often chaotic, pulse trains. In Laser physics, Eqs (1) are quite frequently called the Lorenz-Haken equations, in tribute to Hermann Haken who first recognized the quite surprising analogy between the original Lorenz system, which was derived in the field of fluid-turbulence [1], and the single-mode laser equations [2].

Straightforward linear stability analysis yields an expression for the instability threshold (the level of excitation at which the system bifurcates from stable to unstable behavior) in terms of the field and population inversion decay rates [1-4]

$$\rho_{2th} = \frac{\kappa(\kappa + 3 + \wp)}{\kappa - 1 - \wp} \tag{2a}$$

provided the bad cavity condition

$$\kappa > 1 + \wp \tag{2b}$$

is satisfied.

When the system is excited above such a critical value, the stable steady-state solutions of Eqs (1) transform into unpredictable, quite often complex trajectories. The detailed time-trace features closely depend on the exact values of all three control parameters ρ, κ, and $\wp$.

Let us give some quick survey of the main points that were focused on in hydrodynamics and in laser physics. The first set of control parameters that led Lorenz to introduce the notion of unpredictability in deterministic systems corresponds to κ=10, $\wp$=8/3, and ρ=28. For these parameters, the solution follows a non-periodic flow, describing the so called strange-attractor in phase space. In laser physics, a few systems have been revealed to satisfy the above mentioned bad cavity condition. In such systems, the population-inversion decay-rate $\wp$ is relatively small, and the corresponding solutions develop in the form of regular limit cycles, with increasing periodicity, when the excitation parameter ρ is scanned beyond its instability threshold value ρ_{2th}. Despite a huge amount of numerical investigations that have been reported to characterize the unstable solution of Eqs (1), these never seemed to follow any identifiable standards that would result in the figuring out of any control-parameter chart out of which discernible and predictable information could be extracted. The lone figures that one

may extract from any related literature is that for some control parameter values, the solution is chaotic, while for others it is regular. In between, a series of cascading and bifurcations routes with typical hierarchies of periodic solutions (period one, period two, period four, etc…) depending on how and which of the control parameters is increased or decreased. Indeed, with three control parameters, a complete solution diagram of Eqs (1) would require a three-dimensional representation that takes into account infinite scans of the parameters κ, $\wp$ and ρ. Needless to say, that is a hopeless task to undertake. However, the isomorphic structure of paragraph IV will render such a duty quite easy to carry out. Let us first identify some hidden properties of the Lorenz equations that have never been put forward before.

III. SELF-ORGANIZED SOLUTION-RECURRENCE

The orderly property that we report in this section is described here for the first time. It leaked out after huge amounts of numerical simulations and many years of often "dark-fumbling" in the issue of laser dynamics. These investigations have led us to identify the following property: the ratio of the two decay rates

$$\frac{\kappa}{\wp} = \eta \tag{3}$$

defines an isomorphic class of solutions. This means that for any given couple (κ, $\wp$), a similar solution is obtained if the ratio $\kappa/\wp$ remains unaffected. In other words, replacing κ with $\eta\wp$ in Eqs (1), while scanning over $\wp$ values, for a fixed η, yields the same and identical solution structure.

A wealth of numerical experiments has led us to the same observations and conclusions, i.e. that a fixed η defines a representative class of solutions, for which the value of $\wp$ plays no more role. Therefore, once η is fixed, whatever the variation of $\wp$, the solution structure remains unaltered, as will hereafter be demonstrated with typical examples.

In order to extract conclusive results, we scanned over the values of $\wp$, up to the calculating limits of our lap-top computer, ie $\wp=10^{11}$, and it always appeared that, in all cases, once η is fixed, the structure of the solution remains unaffected, no matter the selected value of $\wp$. The following examples are randomly chosen among countless simulations.

Figure 1 represents two identical period-one orbits, obtained with Eqs (1), for $\eta=30$ and far apart values of κ and $\wp$: a) $\kappa=3$, $\wp=0.1$, b) $\kappa=3.10^{10}$, $\wp=10^9$. These first illustrations undoubtedly exhibit a systematic recurrence of the solutions. Indeed, one may use any pair of (κ, $\wp$) values that lay between those of case a) and case b), as long as these satisfy $\kappa/\wp=\eta=30$, the structure of the period-one solution remains unchanged.

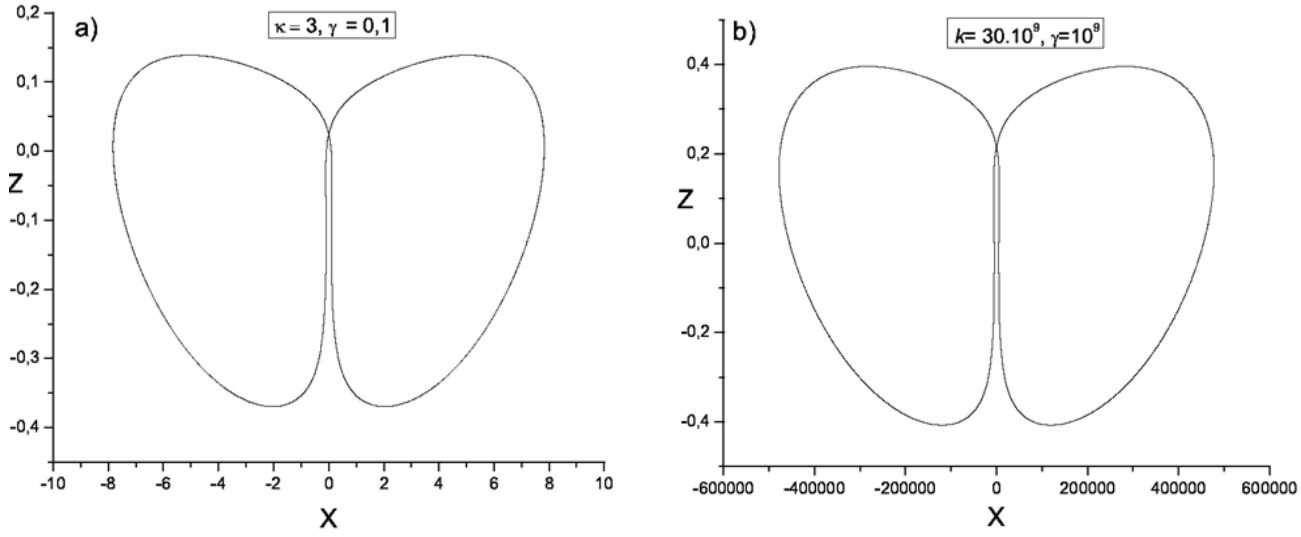

FIG.1 ISOMORPHIC PERIOD-ONE SOLUTIONS OF EQS (1), OBTAINED AT THE INSTABILITY THRESHOLD, WITH EXTREME DECAY-RATE VALUES; A) $\kappa=3$, $\wp=0.1$, AND B) $\kappa=3.10^{10}$, $\wp=10^9$.

A second series of examples, represented in Fig. 2, concerns a period-two orbit in the *(X, Z)* phase-space, obtained with η = 20 and a) κ=3, $\wp$ = 0.15, b) κ=21, $\wp$ = 1.05, and c) κ=20000, $\wp$ = 1000. Again, regardless of the κ and $\wp$ values, the orbit remains the same. Once more, the isomorphic nature of the solutions cannot be ignored.

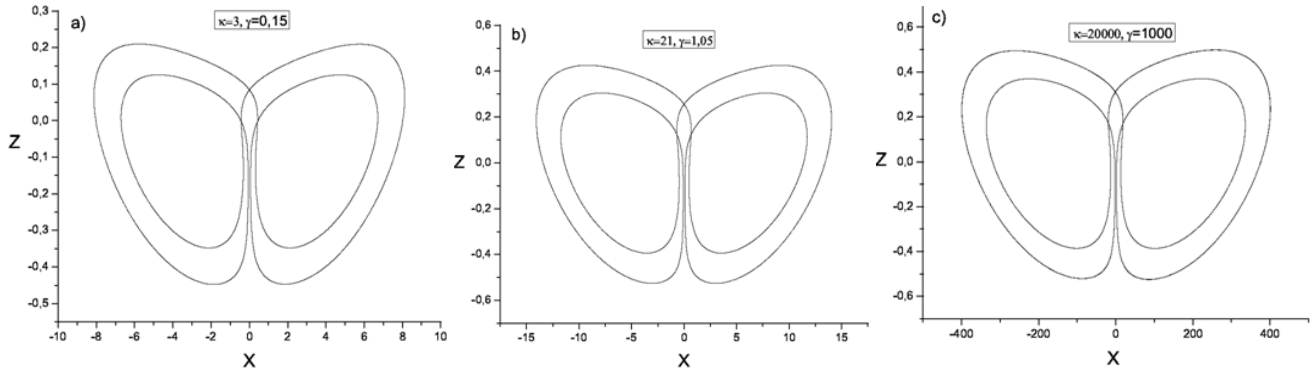

FIG.2 ISOMORPHIC PERIOD-TWO ORBITS, OBTAINED WITH THE SAME, κ / $\wp$ =20, RATIO, AND A) κ =3, $\wp$ =0.15, B) κ =21, $\wp$ =1.05, and c) κ =20000, $\wp$ =1000.

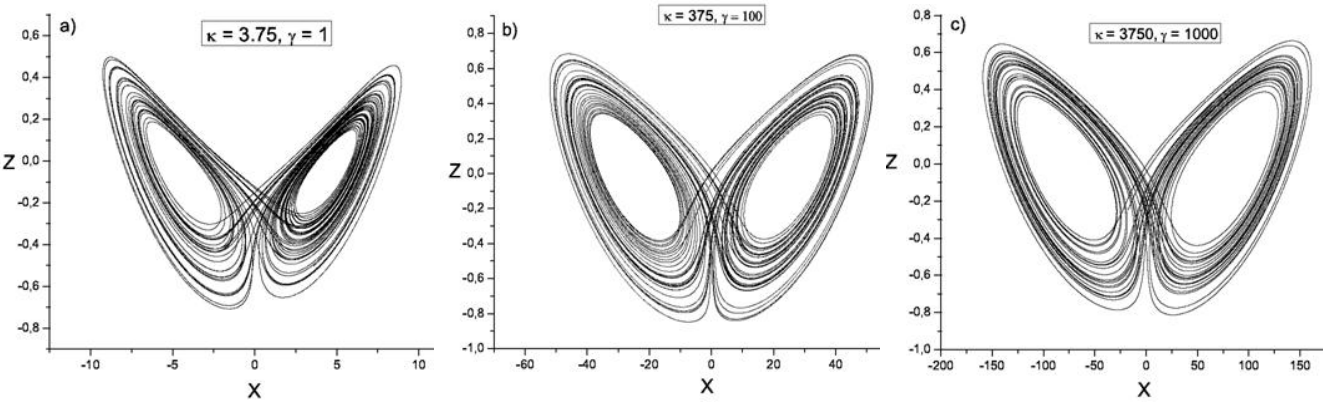

FIG.3 LORENZ ATTRACTOR, AS SIMULATED AT THE INSTABILITY THRESHOLD, WITH A FIXED RATIO κ / $\wp$ = 3.75, AND A) κ =3.75, $\wp$ =1, B) κ =375, $\wp$ =100, AND C) κ =3750, $\wp$ =1000.

As a last example, let us focus on the Lorenz attractor, i.e. the one that corresponds to the original parameters used by Lorenz (κ =10, $\wp$ =8/3), and an instability threshold ρ_{2th} = 24.74. For these parameters, η =3.75. Accordingly, an isomorphic solution is expected with the set (κ =3.75, $\wp$ =1), yielding an instability threshold ρ_{2th} = 16.61; a value which is one-third lower. The phase-space orbits obtained with η =3.75 and increasing κ and $\wp$ values are represented in Fig. 3, for a) κ =3.75, $\wp$ =1, b) κ =375, $\wp$ =100, and c) κ =3750, $\wp$ =1000. Indeed, for these chaotic solutions, one may be entitled to contest the evidence of any isomorphism between these three Lorenz attractors, as compared to the quite convincing examples of periodic solutions. However, since all three attractor follow an erratic path, all three conform to the unpredictable nature that signatures deterministic chaos! Therefore, in view of the remarkable similarities between the periodic examples, undoubtedly, we are entitled to consider that the series of solutions obtained with η =3.75 are all isomorphic to the original Lorenz attractor.

Uncountable examples of such isomorphic solutions have been simulated with fixed values of η, while proportionally scanning over κ and $\wp$. We leave the reader free to choose any other set of parameters, and convince himself, of the recurring nature of the solutions once η is fixed.

Now, let us proceed to the final step and transform Eqs (1) into an isomorphic single-control-parameter system.

IV. A SINGLE-CONTROL-PARAMETER SYSTEM

First, let us note that among the class of isomorphic solutions associated to some fixed η value, there is a particular one which corresponds to $\kappa = \eta$ and $\wp = 1$. For example, the same class of solutions is obtained with the following (κ, $\wp$) sets: (3, 0.1), (6, 0.2), (9, 0.3)….. (30,1) , (60, 2) , (120, 4) ….etc, including the (30,1) set, for which $\kappa = \eta$ =30 and $\wp = 1$. The same analysis is applicable to any series of isomorphic solutions. As a consequence, fixing $\wp$ equal to 1 while replacing κ with η, in Eqs (1), reduces the set of control parameters from three to two, i.e. from (κ, $\wp$, ρ) to (η, ρ). Any solution obtained with the first set may be simulated, with an outright corresponding trajectory, with the second set of control parameters.

Furthermore, our countless numerical experiments (some of which will be specified hereafter) indicate that any solution obtained with a given (η, ρ) set may be identically simulated at the instability threshold, with some other η' value. In other words, at the instability threshold, we retrieve all the wealth of regular and complex solutions that are described with Eqs (1), when any of the three control parameters is scanned over. Replacing the excitation parameter with its instability-threshold expression

$$\rho_{2th} = \frac{\eta(\eta + 4)}{\eta - 2} \tag{4}$$

does not yield any limitation or whatsoever in terms of the solution structures that are obtained directly with Eqs (1). Note that Eq. (4) straightforwardly derives from Eqs (2) and (3).

According to these elements, Eqs (1) transform into

$$\partial_t X = -\eta\{X + \rho_{2th}(\eta)Y\} \tag{5a}$$

$$\partial_t Y = -Y + XZ \tag{5b}$$

$$\partial_t Z = -\{Z + 1 + XY\} \tag{5c}$$

showing an exclusive dependence on the lone control-parameter η. Each value of η now defines a class of isomorphic solutions. As a consequence, at the instability threshold, exclusively related to η, we are left with a single control-parameter. The bad-cavity condition, under which instability sets in, now amounts to $\eta > 2$.

Indeed, for a sealed laser system, the material and cavity decay-rates $\wp$ and κ, respectively, remain fixed. Thus, in order to study the instability hierarchies that take place inside some bad-cavity configured self-pulsing laser, only one parameter, i.e. the excitation level ρ, remains controllable. However, although Eqs (5) exclusively describe the solution structures at the onset of instability, one may always add a quantifying factor, in order to normalize the excitation level with respect to the instability threshold, thus extending its dynamical response to any level of excitation. For such a purpose, the excitation level is parameterized according to

$$\rho = \xi\rho_{2th} \tag{6}$$

transforming Eq. (5) into

$$\partial_t X = -\eta\{X + \xi\rho_{2th}(\eta)Y\} \tag{7}$$

while Eqs (5b) and (5c) remain unchanged. Scanning over ξ amounts to varying ρ. Therefore, the dynamic characteristics may be delimited in terms of ξ values : ξ =1 now defines the instability threshold. So that for ξ <1, the solutions of Eqs (5) are stable, while for $\xi \geq 1$ these are unstable.

It is worth insisting on the fact that the introduction of an additional factor ξ does not add nor subtract any particular solution to the structures that are characteristic of the instability threshold. Such a fact is quite easy to understand, since for any given set of (η, ξ) values, one may always find some matching η ' value for which an isomorphic solution is obtained directly from Eqs (5). The following comparisons illustrate such a property.

As a last convincing example of the isomorphic nature of the solutions of Eqs (1) with those of Eqs (5), which explicitly illustrates the idleness of the factor ξ in Eq. (7), with respect to the dynamic solution structures, let us focus on the period-doubling window, described in [3]. The series of figures represented in pages 66-67 of the reference are the solutions of Eqs (1) that correspond to κ =10, $\wp$ =8/3, and a) ρ =350 b) ρ =260, and c) ρ =216.2. Now, the same series of solutions is obtained with Eqs (7), (5b), and (5c) with η =3.75, and respectively a) ξ =14, b) ξ =7.62, and c) ξ =7.2. The corresponding orbits are shown in Fig 4. A series of identical trajectories are obtained, at the instability threshold (ξ =1) with varying η , which now represents the lone control parameter of the system. The orbits, shown in Fig. 5, were obtained with a) η = 2.1, b) η = 2.14, and c) η =2.141. A first glance comparison between Fig. 4 and Fig. 5 undoubtedly demonstrates a one-to-one equivalence between the three control-parameter equations (Eqs (1)) with the single-control parameter system (Eqs (5)).

We leave to the curious reader the probing of the following example, which we did not include in order to avoid ineffective redundancy: a period-one and a period-two solutions may be simulated with η =30, and, respectively, an excitation level ξ =5, and ξ =7. Meanwhile, their isomorphic solutions may be obtained at the instability threshold (ξ =1), calling for Eqs (5), respectively with η =24.4 and η =23.2.

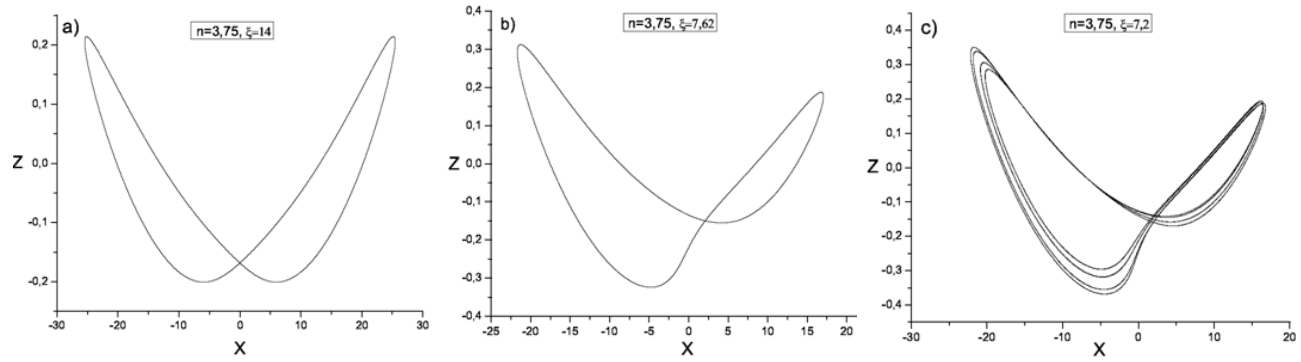

FIG. 4 FIRST FEW ORBITS OF A PERIOD-DOUBLING CASCADE, OBTAINED WITH η =3.75 AND DECREASING EXCITATION PARAMETER; A) ξ =14, B) ξ =7.62, AND C) ξ =7.2.

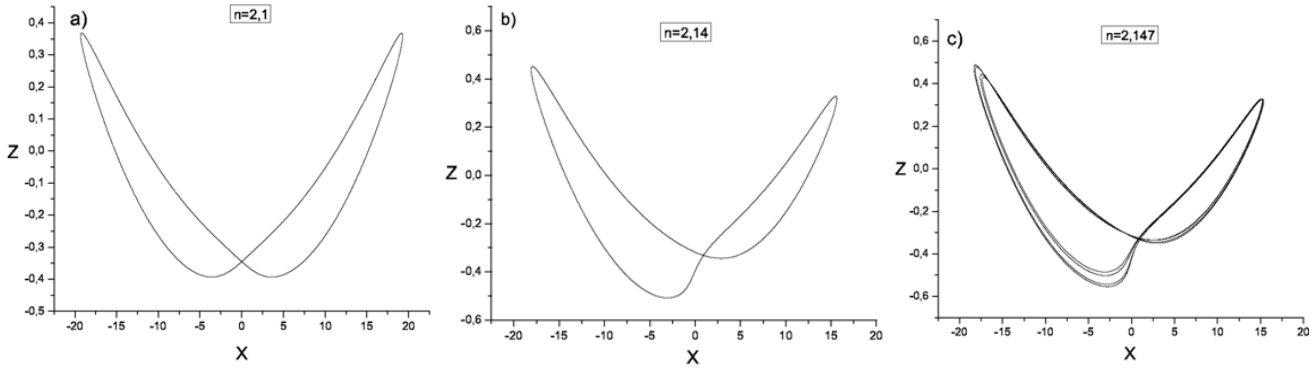

FIG. 5: ISOMORPHIC ORBITS TO THOSE OF FIG. 4, OBTAINED WITH THE SINGLE-CONTROL-PARAMETER EQS (5); A) η =2.1, B) η =2.14, AND C) η =2.147.

A straightforward consequence, which directly concludes the above presented examples, is that one and only one control parameter is needed to describe the full dynamic properties of the Lorenz-Haken equations. These properties are fully contained in the single-control-parameter set (5).

The presence of a single control-parameter in the new set of equations allows for a one-dimensional graphical representation of the distinctive solutions that characterize the nonlinear dynamics. Such a one-dimensional depiction tremendously simplifies the intricate three-dimensional space, which is required to handle the full dynamic properties of Eqs (1).

Such a graph, drawn in Fig. 6, is divided into three main parts, for the purpose of more clarity. It represents a summary of all possible dynamic solutions of Eqs (5) as a function of the lone control parameter η .

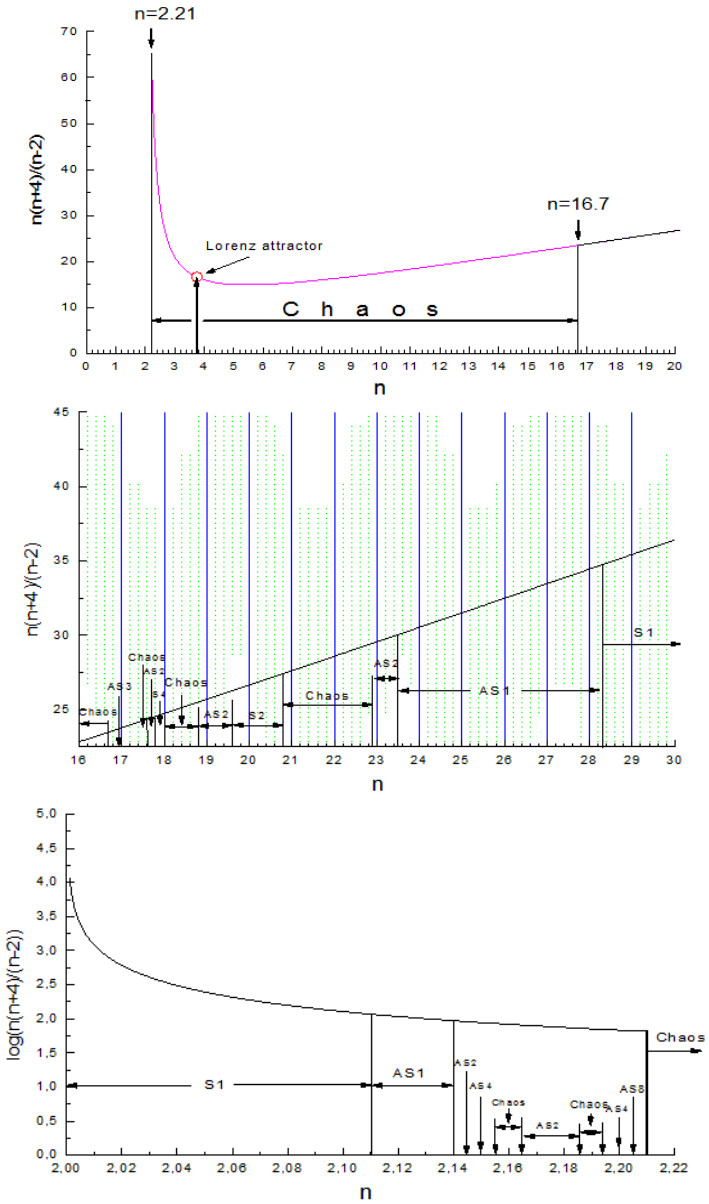

FIG. 6: COMPLETE DIAGRAMS OF THE SOLUTION-STRUCTURES, ILLUSTRATED WITH A ρ_{2th} -VERSUS- η CURVE. THE REPRESENTATION DIVIDES ITSELF INTO THREE MAIN ZONES; A) LARGE CHAOTIC REGION, EXTENDING FROM η =2.21 to η =16.8, b) SERIES OF SYMMETRIC, ASYMMETRIC AND CHAOTIC WINDOWS THAT BECOME LARGER WITH INCREASING η , BEFORE ENDING IN SYMMETRIC PERIOD-ONE SOLUTION, FOR η >28.3, c) SMALL REGION η = [2 - 2.21] WITH DISTINCT WINDOWS, AS INDICATED IN THE GRAPH. NOTE THE LOGARITHMIC SCALE OF THE ρ_{2th} AXIS, IMPOSED BY THE FACT THAT FOR SMALL η VALUES, ρ_{2th} EXHIBITS LARGE VARIATIONS.

A functional summary of the non-linear dynamics, which is rooted in the Lorenz-Haken equations, plainly emerge from the charts of Fig. 6. We first note a large window of persisting chaotic solutions that extends from η=2.21 to η=16.8, and indeed includes the Lorenz attractor, as indicated on the graph. Such a large window, represented in Fig. 6a, clarifies the fact that the Lorenz chaotic attractor is referred to as robust, for it survives any small perturbation inflicted to the coefficients appearing in the Eqs (1). We also notice that chaotic solutions remain robust even under strong η variations, as long as these variations do not step out the chaotic window. Figure 6b indicates that for η>28.3, a symmetric period-one solution is the rule, while the range [16.8, 28.3] contains a series of more or less small windows of Symmetric (S_n) and Asymmetric (AS_n) high-order periodic as well as chaotic solutions. Figure 6c magnifies an interesting, yet very narrow region, merely extending from η = 2.00 to η = 2.21, which also shows distinctive windows of chaotic and asymmetric solutions, along with relatively larger gaps of symmetric (S_1) and asymmetric (AS_1) period-one solutions, as clearly indicated in the graph. Note the logarithmic scale of the ρ_{2th} axis imposed by the very high ρ_{2th} levels associated with small η variations.

Let us note that in practical laser systems, η is the ratio between the cavity and population inversion decay- rates. These two parameters are usually unconnected to one another, yet the graphical representations of Figs 6 may be of great relevance in the design of self-pulsing lasers with predictable yet unsteady outputs, for instance. As a typical example, suppose a given amplifying medium is characterized by a $\wp$=0.5 value, and that we want to observe a chaotic intensity output at the onset of instability. Such a requirement imposes mirror-reflectivity that must comprise cavity decay-rates in the range $1.105 < \kappa < 8.4$, along with the bad cavity condition $\kappa > 1.5$, in order to ensure chaotic trajectories. If, on the contrary, the aim is to prevent chaos, at the onset of instability, the chosen values must lay outside this range. One may indeed extend such an example to any other experimental situation.

It is also expected, from the charts of Figs 6, that our findings be helpful in the field of fluid-turbulence, particularly for quicker set-ups of didactic experiments.

V. CONCLUSION

Leaning on the extraction of, so far unidentified, recurrent-properties of the Lorenz equations, we have constructed and analysed an isomorphic system which carries one single control-parameter only. Such an isomorphic system has been demonstrated to contain the full nonlinear dynamics of the original set, whose unstable solutions are governed by three independent, so far assumed to be unconnected, parameters. Functional graphical-representations, with respect to this lone control-parameter, have been constructed. Such graphs were shown to depict the complete hierarchy of typical windows, each bearing specific solutions. It is expected that this isomorphic system will bring some additional insights to non-linear dynamics studies, both from analytical and experimental points of view.

REFERENCES

[1] E. N. Lorenz, « *Deterministic nonperiodic flow*» J. Atmos. Science 20, 130-141 (1963).

[2] H. Haken, « Analogy Between Higher Instabilities in Fluids and Lasers», Phys. Lett. A 53, 77-78 (1975).

[3] C. Sparrow, «The Lorenz equations: bifurcations, chaos and strange attractors», Applied Mathematical Sciences, vol. 41, Springer-Verlag, Heidelberg, (1982).

[4] B. Meziane, «Pulse structuring in laser-light dynamics: from weak to strong sideband analyses : II – The Lorenz-Haken model», Chap. II, in «Atomic, Molecular and Optical Physics : New Research» Editors: L. T. Chen, Nova Science Publishers, New York pp 61-107(2009), (ISBN :978-1-60456-907-0).

[5] P. Vadasz, « Subcritical transitions to chaos and hysteresis in a fluid layer heated from below», Intern. Journ. Of heat and mass transfer, Vol. 43, N°5, pp 705-724 (2000).

[6] C.O. Weiss et al. « Lorenz-like chaos in NH3-FIR lasers », Infrared Phys. Technol. Vol. 36, N°1, pp 489-512 (1995).

[7] Z. Galias and P. Zgliczy´nski, «Computer assisted proof of chaos in the Lorenz equations», Physica D, Vol. 115, pp. 165–188 (1998).

[8] S. Smale, «Mathematical problems for the next century", Math. Intelligencer», Vol. 20, pp. 7–15 (1998).

[9] W. Tucker, «The Lorenz attractor exists : an auto-validated proof », C. R. Acad. Sci. Paris, t. 328, Série I, p. 1197-1202, (1999).

[10] W. Tucker, «A Rigorous ODE Solver and Smale's 14th Problem», Foundations of Computational Mathematics, Vol. 2, No. 1, pp. 53–117 (2002).

[11] S. Lakshmivaraha, M. E. Baldwin, and Tao Zheng, «Further Analysis of Lorenz's Maximum Simplification Equations», J. Atmos. Sciences, 63 pp2673-2699 (2006).

[12] L.F. Mello, M. Messias , and D.C. Braga, « Bifurcation analysis of a new Lorenz-like chaotic system», Chaos, Solitons & Fractals, Vol. 37, N°4, pp 1244-1255 (2008).

[13] H.R. Dullin, et al. « Extended phase diagram of the Lorenz model », Int. J. of Bifurcation and Chaos, Vol. 17 pp 3013-3033 (2007).

[14] TS Zhou, et al., « The complicated trajectory behaviours in the Lorenz equation », Chaos Solitons & Fractals, Vol. 19, N° 4 pp 863-873 (2004).

[15] B. Meziane and S. Ayadi, «Third-order laser-field-expansion analysis of the Lorenz–Haken equations», Optics Commun. Vol. 281, 15-16, 4061-4067 (2008).

[16] B. Meziane, *«Non-linear structure of the light-intensity-output versus pump-input characteristics in self-pulsing lasers»*, Optical and Quantum Electronics, 46:305–317 (2014) - doi: 10.1007/s11082-013-9761-6.